MODELING OF NO FORMATION BASED ON ILDM REDUCED CHEMISTRY

J. NAFE AND U. MAAS

Institut für Technische Verbrennung
Stuttgart University
Pfaffenwaldring 12
D-70569 Stuttgart, Germany

The reduction of NO formation is a challenging task in view of a clean operation of combustion processes. For the mathematical modeling of turbulent combustion processes, it is desirable to devise reduced schemes for the chemical kinetics which allow a reliable description of kinetically controlled processes such as NO formation. This work focuses on an extension of the method of intrinsic low-dimensional manifolds (ILDM) in order to include NO chemistry, which is well known to be governed by very slow chemical reactions. For the generation of simplified chemical reaction mechanisms, this behavior permits the assumption that these processes as nearly frozen in large parts of the reaction domain. At first, the chemical dynamics of the NO system are analyzed. Based on this analysis, a method is devised which allows the description of NO formation in the context of ILDM-reduced chemistry. Sample calculations of NO formation in CH_4/air flames verify the approach, and the application in general computational fluid dynamics calculations is discussed.

Introduction

In recent years, considerable progress has been made in the development of detailed kinetic schemes for combustion including pollutant formation kinetics [1,2]. Detailed kinetics is, however, in most cases computationally prohibitive for turbulent reactive three-dimensional flows [3]. This is caused by the large number of chemical species (sometimes more than 1000), which react in several thousand reactions, for example, in low-temperature oxidation of higher hydrocarbons [4]. To decrease the computational effort, several methods for the reduction of the detailed chemical mechanisms have been devised (see, e.g., Refs. [5–7]). One of these techniques is the method of intrinsic low dimensional manifolds (ILDM) [8,9]. It has been shown to be an efficient tool for the automatic generation of reduced mechanisms, which describe the chemical dynamics by a small number of progress variables only, nevertheless capturing the essential characteristics of the dynamics of the chemical reaction.

The concept of ILDM is based on an analysis of the timescales of chemical systems. The chemical timescales cover several orders of magnitude (10^{-10} to 10^0 s). The fast chemical processes can be decoupled from the reaction system, and as a result, reduced mechanisms are obtained, which contain typically two to four reactive variables only. This decoupling of the fast timescales and the generation of reduced mechanisms has been used in several previous papers by various groups (see, e.g., Refs. [8–15]).

One problem in the concept of ILDM is the fact that all slow chemical processes have to be accounted for; that means each slow process enters the ILDM as an additional dimension. This is a disadvantage, in particular, if NO formation (which is a slow process) has to be accounted for. Thus, it is desirable to extend the ILDM concept such that slow chemical processes can also be decoupled. This can be done by treating slow chemical processes as frozen in parts of the composition space, while allowing them to become important in other domains (e.g., close to the chemical equilibrium). Such an extension of the ILDM concept will be presented in the following.

The next sections of this paper focus at first on the description of the dynamics of the NO system as an example of a slow chemical subsystem. Then, the decoupling of the slow timescales within the concept of the ILDM method will be considered. Finally, we conclude with a comparison of the detailed and reduced mechanism and a discussion of the results obtained.

Dynamics of Chemically Reacting Flows

In chemically reacting systems, the composition state is characterized by the vector $\boldsymbol{\psi} = (h, p, w_i/M_i)^T$, where h denotes the enthalpy, p the pressure, w_i the species mass fractions, and M_i the molar masses. In a typical combustion process, the dynamics of the scalar field is governed by the equation [8,10]

λ = 1/τ (1/s)
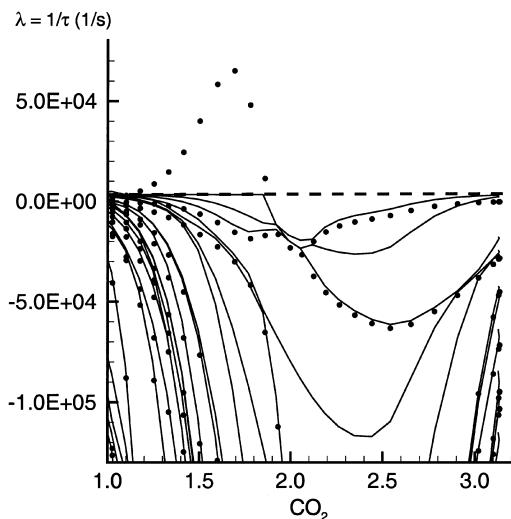
FIG. 1. Typical timescales of a laminar free flat flame under adiabatic, isobaric, and homogeneous conditions. The flame is calculated for a stoichiometric CH_4/air system using detailed chemistry including NO formation (lines) and omitting NO formation (symbols).

$$\frac{\partial \boldsymbol{\psi}}{\partial t} = \mathbf{F}(\boldsymbol{\psi}) + \boldsymbol{\Xi}(\boldsymbol{\psi}, \nabla\boldsymbol{\psi}, \Delta\boldsymbol{\psi}) = \mathbf{F}(\boldsymbol{\psi})$$

$$+ \mathbf{v} \cdot \mathrm{grad}\boldsymbol{\psi} + 1/\rho \cdot \mathrm{div}\mathbf{D} \cdot \mathrm{grad}\boldsymbol{\psi} \quad (1)$$

where $\mathbf{F}(\boldsymbol{\psi})$ denotes the vector of source terms, $\mathbf{v}$ the velocity, ρ the density, and $\mathbf{D}$ the matrix of transport coefficients. This evolution of the scalar field is governed by a variety of different timescales which stem from the chemical source terms and the physical processes.

As an example, the timescales introduced by the chemical source term of a laminar free flame will be analyzed. The flame and all further results are based on a stoichiometric CH_4/air mixture with a specific enthalpy of $h = -25.69 \cdot 10^4$ J/kg (corresponding to an unburnt temperature $T_u = 298$ K) and a pressure of $p = 1$ bar. In order to simplify the treatment, Lewis number $Le = 1$ and equal diffusivities are assumed, but the method proposed can be applied to the general case, too. The mechanism includes NO chemistry and contains 52 chemical species reacting in 573 reactions [2]. It involves the important rection paths of the Zeldovich mechanism, the prompt NO formation, and the N_2O route. Due to $Le = 1$ and the equal diffusivities, the timescales of the evolution of enthalpy, pressure, and element mass fractions (C, H, O, N) are infinite. The remaining 48 timescales cover, as mentioned above, several orders of magnitude. Fig. 1 shows the time scales τ_i for a flame calculation including NO formation (lines) and for a flame where the NO chemistry has been neglected (symbols). The eigenvalues

($\lambda_i = 1/\tau_i$) of the Jacobian F_ψ are plotted against the coordinate $\phi_{CO_2} = w_{CO_2}/M_{CO_2}$, which acts as a reaction progress variable and is 0 in the unburnt mixture and ≈ 3.12 mol/kg at chemical equilibrium (only the eigenvalues smallest in magnitude are plotted). Several points are worthy of note. First, the NO reactions introduce new timescales (lines without symbols). In particular, one very slow timescale is introduced (dashed line in Fig. 1). But we can also see that the original timescales of the combustion system without NO formation are (at least for the slow timescales in the figure) almost unaltered. Note that the part of the figure with $\phi_{CO_2} < 2$ mol/kg corresponds to the low-temperature regime, where timescale splitting within the concept of ILDM is difficult and the dynamics is governed by diffusive processes.

NO chemistry gives rise to additional slow timescales and, within the concept of ILDM, this necessitates the use of additional progress variables. Thus, the fundamental question is whether it is possible to decouple the slow processes, too. That this should be possible can be seen, for example, from the fact that postprocessing schemes for NO formation yield good results [16].

For the following, let us have a look at the pure dynamics of the chemical reaction system only, neglecting physical processes such as diffusion ($\boldsymbol{\Xi} = 0$ in equation 1). Chemical reaction is governed by a movement along trajectories toward chemical equilibrium. Chemical equilibrium is a point in the reaction space, which is defined by the enthalpy, the pressure, and element composition only. If these values are held constant, every point, independent of the starting values, relaxes into the same chemical equilibrium. Before chemical equilibrium is reached, the trajectories have merged on a one-dimensional manifold, and before this manifold is reached, they have already relaxed onto a two-dimensional manifold and so on. In Fig. 2, several trajectories are plotted for different initial values. The trajectories are calculated using detailed chemistry. Trajectories of the same color correspond to the same initial concentration of NO. It can be seen that trajectories with the same initial NO concentration all relax onto the same one-dimensional line, until the equilibrium of CO_2 and H_2O is almost achieved. Afterward, the chemical dynamics moves along the NO coordinate into the chemical equilibrium. Fig. 2 shows also that all trajectories, independent of their initial values, relax onto this slow manifold which characterizes NO formation. As a result of this behavior, it can be seen that, in principle, the simulation of NO requires an additional coordinate. But, on the other hand, in technical systems, the initial values of NO are typically fixed (e.g., there is no NO in the fuel or in the air). This means that typically only the black trajectories are relevant and, up to a state close to equilibrium, NO acts as a *frozen* variable which remains constant.
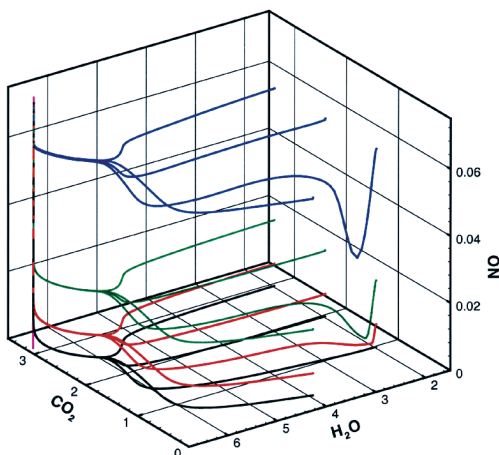
FIG. 2. Several homogeneous reactor calculations and a one-dimensional ILDM (purple line) for a stoichiometric CH_4/air system are calculated using detailed chemistry including NO formation They are plotted in a projection of the state space in CO_2/H_2O/NO coordinates. The species concentrations are in units of $[w_i/M_i]$ mol/kg.

It has already been shown that new timescales are introduced by NO chemistry, but the original ones are typically not influenced. The next important question for understanding the dynamics of the NO system is: How does the NO chemistry influence the original CH_4 system? To give an idea of the answer to this question, Fig. 3 shows two two-dimensional projections of the reaction space into the coordinates of O_2–CO_2 and H–CO_2. The trajectories shown are the same as in Fig. 2. It can be seen that all trajectories, varying in the initial values of the NO system only, have almost the same evaluation with respect to the variables of the original system (CH_4 chemistry only). For projections into coordinates spanned by other species of the CH_4/air system (not shown here), a similar behavior is obtained. Thus, it can be seen that the original system is almost not influenced by the additional reactions for the NO formation. This confirms the well-known fact that NO formation can be modeled with a postprocessing step [16], based on ILDMs including CH_4 chemistry only.

Decoupling of the NO Chemistry Within the ILDM Concept

From Fig. 2 it can be seen clearly that the slowest chemical process remains frozen for a long time. This corresponds to the fact that if one starts from initial conditions without any species of the NO-formation mechanism, the system can, for a long time, be described by the pure CH_4 system without any nitrogen-containing species (except for N_2). Thus, it
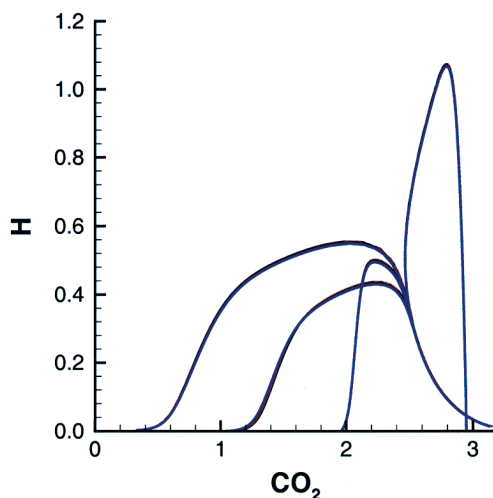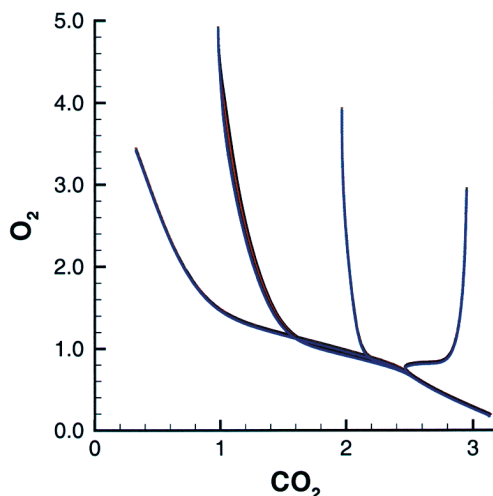
FIG. 3. Several trajectories of chemical kinetics for a stoichiometric CH_4/air system using detailed chemistry including NO formation. Plots of projections of the state space in O_2/CO_2 and H/CO_2 coordinates, respectively. The species concentrations in units of $[w_i/M_i]$ = mol/kg.

is important to investigate how an ILDM for the CH_4 combustion chemistry is influenced by addition of NO chemistry.

Let the original chemical system (say CH_4 combustion) be governed by the system

$$\frac{\partial \boldsymbol{\psi}}{\partial t} = \mathbf{F}(\boldsymbol{\psi}) \tag{2}$$

and let the additional species introduced by the NO system be denoted by $\boldsymbol{\eta}$. If the additional reactions
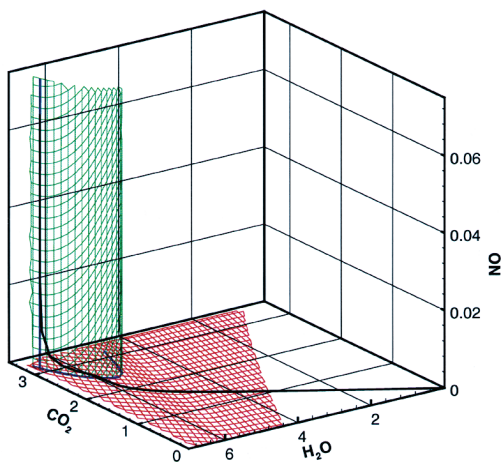
FIG. 4. One-dimensional ILDMs (blue lines), two-dimensional ILDMs (red and green mesh) generated using mechanisms containing CH_4 and CH_4 + NO chemistry. In addition, a flame trajectory using detailed CH_4 + NO chemistry is plotted. Projection of the state space into CO_2/ H_2O/NO coordinates, species concentrations in units of $[w_i/M_i] = $ mol/kg.

contribute only marginally to the rates of the original system, then the augmented system is governed by

$$\frac{\partial \boldsymbol{\psi}}{\partial t} = \mathbf{F}(\boldsymbol{\psi}) + \varepsilon \cdot \mathbf{G}(\boldsymbol{\psi}, \boldsymbol{\eta}) \qquad (3)$$

$$\frac{\partial \boldsymbol{\eta}}{\partial t} = \mathbf{H}(\boldsymbol{\psi}, \boldsymbol{\eta}) \qquad (4)$$

where ε is a small number, and $\mathbf{H}(\boldsymbol{\psi}, \boldsymbol{\eta})$ and $\mathbf{G}(\boldsymbol{\psi}, \boldsymbol{\eta})$ correspond to additional source terms introduced by the additional reactions. For $\varepsilon \to 0$ it can be shown (see Appendix) that the ILDM for this augmented system is given by

$$\tilde{\mathbf{Z}}_f \, \mathbf{F}(\boldsymbol{\psi}) = 0 \qquad (5)$$

$$\mathbf{x}_f \tilde{\mathbf{Z}} \mathbf{F}(\boldsymbol{\psi}) + \tilde{\mathbf{W}}_f \mathbf{H}(\boldsymbol{\psi}, \boldsymbol{\eta}) = 0 \qquad (6)$$

where equation 5 is the original definition of the ILDM of the unperturbed system and equation 6 denotes additional conditions for the decoupling of fast processes of the NO system. The $(n_f \times n)$-dimensional matrix $\tilde{\mathbf{Z}}_f$ denotes the left invariant subspace of the original system associated with the fast relaxing timescales, the matrix $\tilde{\mathbf{W}}_f$ is the left invariant subspace of the additional processes, and the matrix product $\mathbf{x}_f \tilde{\mathbf{Z}}$ is a projection of the matrix $\tilde{\mathbf{Z}}_f$ (see appendix for a detailed description). This means that the overall ILDM can be represented as

$$\boldsymbol{\psi} = \boldsymbol{\psi}(\boldsymbol{\theta}) \wedge \boldsymbol{\eta} = \boldsymbol{\eta}(\boldsymbol{\theta}, \xi) \qquad (7)$$

where $\boldsymbol{\theta}$ denotes the controlling variables of the

original system and ξ denotes the additional controlling variables of the NO system. The left part of equation 7 denotes the condition for the ILDM of the original system, the right part represents the solution of equation 6, that is, it defines the state relations introduced by the additional fast reactions of the added subsystem. Note that the existence and uniqueness of solutions can be investigated based on the characteristics of the governing equations 5 and 6. An *a priori* investigation is difficult, but information from the numerical solution algorithm can be used to obtain the characteristics of the solution of equation 7.

This behavior can be understood best by a simple test example shown in Fig. 4. This figure shows two one-dimensional ILDMs (blue lines), which are generated using the original and the complete mechanism. This means that they correspond to reduced schemes which describe only the slowest chemical processes (NO formation) in the full mechanism, and slow completion of combustion in the case without NO chemistry. Two two-dimensional ILDMs are also plotted. One of the two-dimensional ILDMs (red mesh) describes CH_4 chemistry only. The other two-dimensional ILDM (green mesh) involves the complete reaction mechanism and characterizes the dynamics in the region, where the slow timescales cannot be assumed to be frozen. This ILDM includes both one-dimensional ILDMs. Additionally, a flame trajectory of a laminar free flat flame using detailed chemistry is plotted into Fig. 4. At first, the trajectory lies in the two-dimensional ILDM without NO chemistry (red mesh), then within the two-dimensional ILDM including NO chemistry (green mesh), and afterward within the corresponding one-dimensional ILDM (blue line). If the one-dimensional ILDM (blue line) characterizing slow NO formation is reached, the chemical dynamics is restricted to a movement along this manifold until the chemical equilibrium is achieved.

This behavior clarifies the strategy to account for NO chemistry within the ILDM concept. In the early phases of combustion, the ILDM of the system without NO chemistry (or the ILDM of the complete system with NO chemistry frozen) can be used and close to the equilibrium we have to *switch* to the ILDM including NO chemistry. Although an additional slow process has then to be taken into account, the required dimension of the ILDM is not increased because, on the other hand, one process which could not be decoupled far from the equilibrium now has become fast and can be decoupled. There are several possible ways to implement this strategy.

One simple method is to define domains where one or the other ILDM has to be used and to perform a real *switch* of the variables in the computational fluid dynamics (CFD) calculation.
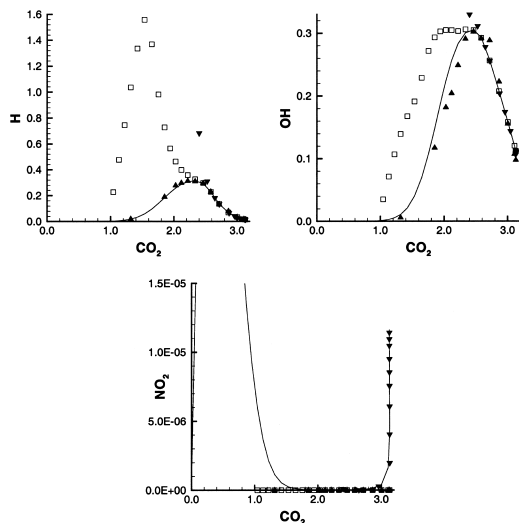
FIG. 5. Comparison of the reduced and detailed mechanism. CO_2 is used to describe the reaction progress Lines, detailed mechanism; $\square$, two-dimensional ILDM using pure CH_4 chemistry; $\blacktriangledown$, two-dimensional ILDM using CH_4 + NO chemistry; $\blacktriangle$, three-dimensional ILDM using pure CH_4 chemistry. The species concentrations are in units of $[w_i/M_i]$ = mol/kg.

The other method is based on the observation that typically only parts of the manifold are actually accessed in the calculation. Thus, it is possible to generate (based on the two ILDMs) one unique representation of a *combined* ILDM. Then the *combined* m-dimensional ILDM is projected onto the new coordinates. For the example considered here, the resulting m-dimensional hyperplane might be parameterized by a linear combination of the coordinates ϕ_{CO_2} and ϕ_{NO} and ϕ_{H_2O} as second coordinate.

The example presented describes NO formation for a stoichiometric mixture, only. This raises the question, what will happen if rich mixtures are considered? For such conditions prompt NO formation exerts an important influence on the overall chemical dynamics (not only the NO chemistry). Therefore, a separation into pure hydrocarbon chemistry and NO chemistry is not possible. This means at least three reaction progress variables are necessary. But, according to the higher accuracy of a three-dimensional ILDM, this is desirable anyway (see Fig. 5 which is discussed in the next section).

Let us return to the evolution equation (see equation 1) for the scalar field. Within the concept outlined above, this equation system can be simplified by projecting the equation onto the ILDMs of given dimension (see, e.g., Refs. [8,10,17]), and in addition, freezing the slow chemical processes.

The resulting m-dimensional evolution equation is then given by

$$\frac{\partial \boldsymbol{\theta}}{\partial t} = \mathbf{S}(\boldsymbol{\theta}, \xi) + \boldsymbol{\Pi}(\boldsymbol{\theta}, \nabla\boldsymbol{\theta}, \Delta\boldsymbol{\theta}, \xi, \nabla\xi, \Delta\xi) \quad (8)$$

where $\boldsymbol{\theta} = (\theta_1, \ldots \theta_m)^T$ is the m-dimensional vector of slow variables, $\xi = (\xi_1, \ldots \xi_{n-m-n_f})^T$ is the $(n - m - n_f)$-dimensional vector of variables with locally negligible (frozen) chemistry, $\mathbf{S}$ denotes the chemical source term, $\boldsymbol{\Pi}$ the projected term of physical processes, and n_f the number of fast decoupled processes.

It should be noted that this concept can also be applied to other slow chemical processes in order to reduce the necessary dimension of the ILDM. As can be seen in the previous examples, high dimensions of the ILDMs can thus be avoided if slow processes are temporarily decoupled from the system simultaneously to the decoupling of fast timescales.

Results and Discussion

In order to validate the concept presented above, results obtained using the detailed and reduced mechanism are compared. This is done for the free flat flame already presented. Detailed results correspond to the results obtained from a calculation based on the detailed reaction mechanism (see above) and results using reduced chemistry correspond to the concentrations of the chemical species predicted by the different ILDMs. The results are presented in Fig. 5. Species concentrations are plotted versus CO_2, which acts as a reaction progress variable and allows a clearer representation than a plot against the spatial coordinate. The line denotes the detailed results, $\square$ correspond to results obtained using the two-dimensional ILDM without NO chemistry, $\blacktriangledown$ represents the two-dimensional ILDM containing the complete mechanism, and $\blacktriangle$ belongs to a three-dimensional ILDM using CH_4 chemistry only.

It can be seen that in large parts of the flame the use of a three-dimensional ILDM yields a high accuracy. Close to the equilibrium (in the zone behind the flame front), even a two-dimensional ILDM yields good results. Quite close to equilibrium, the two-dimensional ILDM including NO chemistry yields accurate results. NO_2 is, for example, predicted correctly by these ILDMs. Note that the deviation in the cold part of the flame can of course not be predicted by such a low-dimensional model. On the other hand, this initial formation of NO_2 contributes in a negligible way to the overall NO_x formation. The calculations also confirm that the rate of formation of NO is predicted correctly.

These results demonstrate that the decoupling of the fast timescales from the reaction system and the assumption of considering the NO chemistry in large parts of the flame as frozen are valid. With increasing reaction progress, the slow timescales become more important and have to be taken into account.

In order to consider the slow timescales, a new progress variable has to be used, whereas other processes can be neglected because they have become fast. This means that NO chemistry can be accounted for in a accurate way without increasing the overall required dimension of the ILDM.

Conclusions

The dynamical behavior of the NO system discussed in this work permits slow chemical processes to be considered frozen within the concept of ILDM within large domains of the composition space. But the slow timescales become important and cannot be neglected any longer in other domains (close to equilibrium). In general, mechanisms containing NO chemistry can be reduced with the ILDM concept. For the implementation of the reduced mechanism in CFD codes, however, different strategies are possible. One method simply uses more progress variables than used for the underlying ILDMs without NO chemistry, but this causes an increase of the computational effort. On the other hand, in the domain where the very slow chemical processes become important, some of the considered timescales have already relaxed and can be decoupled. This means that new progress variables have to be used for the additional slow timescales, whereas others have become negligible, because the corresponding timescales have become fast. Therefore, the number of progress variables remains constant. The method has been demonstrated for the specific example of CH_4 combustion including NO formation, but the strategy can also be used to decouple other slow subsystems.

Appendix

Let a reaction system be given by

$$\frac{\partial \psi}{\partial t} = F(\psi) \tag{9}$$

Now let us assume that we add a new submechanism which adds the n_a new chemical species, and assume that the perturbation of the original system is small. Then we obtain

$$\frac{\partial \psi}{\partial t} = F(\psi) + \varepsilon G(\psi, \eta) \tag{10}$$

$$\frac{\partial \eta}{\partial t} = H(\psi, \eta) \tag{11}$$

and the Jacobian J of the coupled system is given by

$$J(\psi, \eta) = \begin{pmatrix} F_\psi + \varepsilon G_\psi & \varepsilon G_\eta \\ H_\psi & H_\eta \end{pmatrix} \tag{12}$$

and for $\varepsilon \to 0$ the Jacobian J of the augmented system is given by

$$J(\psi, \eta) = \begin{pmatrix} F_\psi & 0 \\ H_\psi & H_\eta \end{pmatrix} \tag{13}$$

Furthermore, we perform a subspace decomposition such that

$$\begin{pmatrix} \tilde{Z}_s \\ \tilde{Z}_f \end{pmatrix} F_\psi = \begin{pmatrix} N_s & 0 \\ 0 & N_f \end{pmatrix} \begin{pmatrix} \tilde{Z}_s \\ \tilde{Z}_f \end{pmatrix} \begin{pmatrix} \tilde{Z}_s \\ \tilde{Z}_f \end{pmatrix}^{-1} = Z \tag{14}$$

and

$$\begin{pmatrix} \tilde{W}_s \\ \tilde{W}_f \end{pmatrix} H_\eta = \begin{pmatrix} M_s & 0 \\ 0 & M_f \end{pmatrix} \begin{pmatrix} \tilde{W}_s \\ \tilde{W}_f \end{pmatrix} \tag{15}$$

where $\lambda_i^{real} (N_s) < \lambda_j^{real} (N_f)$ and $\lambda_i^{real} (M_s) < \lambda_j^{real} (M_f)$ for all i, j (see Ref. [18]). A lengthy calculation shows that the left invariant subspaces of the Jacobian J associated with N_f and M_f are given by

$$(\tilde{Z}_f \; 0) \quad \text{and} \quad (x_f \tilde{Z} \; \tilde{W}_f) \tag{16}$$

where x_f solves the Sylvester equation

$$M_f x_f - x_f \begin{pmatrix} N_s & 0 \\ 0 & N_f \end{pmatrix} = \tilde{W}_f H_\psi Z \tag{17}$$

This means that the ILDM of the augmented system is given by

$$\tilde{Z}_f F(\psi) = 0 \tag{18}$$

$$x_f \tilde{Z} F(\psi) + \tilde{W}_f H (\psi, \eta) = 0 \tag{19}$$

and thus the ILDM is given by the ILDM in the original system augmented by additional constraints for the new variables. From that it follows that a projection of the global new ILDM into the space of the old variables corresponds to the ILDM of the original system.

REFERENCES

1. Warnatz, J., *Proc. Combust. Inst.* 24:553–579 (1992).
2. Warnatz, J., Maas, U., and Dibble, R. W., *Combustion,* Springer-Verlag, Berlin, 1996.
3. Pope, S. B., *Proc. Combust. Inst.* 23:591–612 (1990).
4. Chevalier, C., "Entwicklung eines detaillierten Reaktionsmechanismus zur Modellierung der Verbrennungsprozesse von Kohlenwasserstoffen bei Hoch- und Niedertemperaturbedingungen," Ph.D. thesis, Institut für Technische Verbrennung, Universität Stuttgart, 1993.
5. Smooke, M. D., (ed.), *Reduced Kinetic Mechanisms and Asymptotic Approximations for Methane-Air Flames,* Lecture Notes in Physics 384, Springer, Berlin, 1991.
6. Peters, N., and Rogg, B., *Reduced Kinetic Mechanisms for Applications in Combustion Systems,* Springer, Berlin, 1993.

7. Tomlin, A. S., Turanyi, T., and Pilling, M. J., "Mathematical Tools for the Construction, Investigation and Reduction of Combustion Mechanisms," in *Comprehensive Chemical Kinetics 35: Low-Temperature Combustion and Autoignition* (M. J. Pilling, ed.), Elsevier, Amsterdam, 1997.

8. Maas, U., and Pope, S. B., *Combust. Flame* 88:239–264 (1992).

9. Maas, U., and Pope, S. B., *Proc. Combust. Inst.* 24:103 (1992).

10. Maas, U., and Pope, S. B., *Proc. Combust. Inst.* 25:1349–1356 (1994).

11. Blasenbrey, T., Schmidt, D., and Maas, U., *Proc. Combust. Inst.* 27:505–511 (1998).

12. Blasenbrey, T., and Maas, U., *Proc. Combust. Inst.* 28:1623 (2000).

13. Eggels, R. L. G. M., and de Goey, L. P. H., *Combust. Flame* 100:559–570 (1995).

14. Gicquel, O., Thévenin, D., Hilka, M., and Darabiha, N., *Combust. Theory Modelling* 3:479–502 (1999).

15. Correa, C., Niemann, H., Schramm, B., and Warnatz, J., *Proc. Combust. Inst.* 28:1607 (2000).

16. Eggels, R. L. G. M., and de Goey, L. P. H., *Combust. Flame* 107:65–71 (1996).

17. Maas, U., "Mathematical Modeling of the Coupling of Chemical Kinetics with Laminar and Turbulent Transport Processes," in *Computational Fluid and Solid Mechanics* (K. J. Bathe, ed.), Elsevier, Amsterdam, 2001, p. 1304.

18. Maas, U., *Comput. Visual. Sci.* 1:69–82 (1998).

COMMENTS

Stephen B. Pope, Cornell University, USA. It seems that at the junction of the two manifolds, the compositions are continuous but not differentiable. Do these cause problems in the diffusion term in the flame equations?

Author's Reply. Indeed, the junction of the two manifolds typically leads to a nondifferentiable mapping. On the other hand, in a typical application, the manifold is tabulated, and subsequently the properties of points on the manifold are evaluated using a table look-up with a multilinear interpolation which itself does not yield differentiable results. Numerical experiments have shown that (due to numerical diffusion) this typically does not cause problems in the evaluation of the diffusion term. In addition there is also the possibility to approximate the joint manifold by a continuous and differentiable manifold which can, for example, be constructed based on an algorithm that evolves the ILDM toward an inertial manifold, which is by definition continuous and differentiable [1].

REFERENCE

1. Nafe, J., and Maas, U., unpublished manuscript.